PHYSICAL REVIEW D

PARTICLES, FIELDS,
GRAVITATION, AND COSMOLOGY

THIRD SERIES, VOLUME 46, NUMBER 2 15 JULY 1992

ARTICLES

Proposed new determination of the gravitational constant G and tests of Newtonian gravitation

Alvin J. Sanders and W. E. Deeds
Department of Physics and Astronomy, The University of Tennessee, Knoxville, Tennessee 37996
(Received 16 August 1991)

The first "constant of nature" to be identified, Newton's constant of universal gravitation G, is presently the least accurately known. The currently accepted value $(6.672\,59\pm0.000\,85)\times10^{-11}$ $m^3kg^{-1}s^{-2}$ has an uncertainty of 128 parts per million (ppm), whereas most other fundamental constants are known to less than 1 ppm. Moreover, the inverse-square law and the equivalence principle are not well validated at distances of the order of meters. We propose measurements within an orbiting satellite which would improve the accuracy of G by two orders of magnitude and also place new upper limits on the field-strength parameter α of any Yukawa-type force, assuming a null result. Preliminary analysis indicates that a test of the time variation of G may also be possible. Our proposed tests would place new limits on $\alpha=\alpha_5(q_5/\mu)_1(q_5/\mu)_2$ for characteristic lengths Λ between 30 cm and 30 m and for $\Lambda>1000$ km. In terms of the mass m_b of a vector boson presumed to mediate such a Yukawa-type force, the proposed experiment would place new limits on α for 7×10^{-9} eV$<m_bc^2<7\times10^{-7}$ eV and for $m_bc^2<2\times10^{-13}$ eV. Two distinct tests of the inverse-square law, one employing interactions at intermediate distances and having a peak sensitivity if Λ is a few meters (i.e., $m_bc^2\sim10^{-7}$ eV), and the other employing interactions at longer distances and having a peak sensitivity for $\Lambda\sim R_{\rm Earth}$ ($m_bc^2\sim3\times10^{-14}$ eV), would both place limits of 10^{-5} to 10^{-6} on α. These interactions also provide tests of the equivalence principle (Eötvös' experiment). The intermediate-distance interaction would test the equivalence principle to 5 parts in 10^7 for $\Lambda>5$ m ($m_bc^2<4\times10^{-8}$ eV), while the longer-distance interaction would test the equivalence principle to 4 parts in 10^{13} for $\Lambda>R_{\rm Earth}$ ($m_bc^2<3\times10^{-14}$ eV). Specifically, we propose to observe the motion of a small mass during the encounter phase of a "horseshoe" orbit—that is, in the vicinity of its closest approach to a large mass in a nearly identical orbit. The essential aspect of the interaction of the two bodies during the encounter is an exchange of energy, and we call the proposed method the "satellite energy exchange" (SEE) method. Successful application of the SEE method to gravity measurements will depend on the particular experimental design, including the configurations of the test bodies, the characteristics of the systems for maneuvering the test bodies and the satellite, and the choice of orbital parameters, which are described below. We are not aware of any existing or proposed method which approaches the accuracy of the SEE method.

PACS number(s): 04.80.+z, 04.90.+e, 06.20.Jr

I. INTRODUCTION

Much of the difficulty in gravitational measurements arises from the extreme weakness of the gravitational force between the test bodies compared to other forces acting on the bodies [1–4], such as electromagnetic effects and instrumental friction. Space is attractive for gravitation measurements because it has the potential to be relatively "clean" and free of the influences which necessarily cloud the interpretation of terrestrial experiments. In this respect we follow the lead of other investigators who have proposed measuring G in space [5]. The satellite energy exchange (SEE) method would measure the gravitational interaction between two test bodies by placing them in nearly identical Earth orbits and treating their interaction by *orbital perturbation techniques,* which

historically have enjoyed unsurpassed accuracy. A metallic capsule enclosing the test bodies would shield them from other forces, such as atmospheric drag and solar radiation pressure, ensuring that their mutual gravitational attraction is much larger than any other effects. Interferometry would allow very accurate measurements of the motion of the test bodies and, hence, of the gravitational force between them. The accuracy of the G determination by the SEE method is expected to be limited by the accuracy with which the mass of the larger test body can be related to the standard kilogram.

The SEE interaction itself is a novel choice of test-body dynamics, and it is critical for exploiting the obvious inherent advantages of the space environment. Moreover, our proposed experimental method goes to great lengths to ensure that the capsule will be thermally and mechanically quiet, with particular care to avoid capsule distortion by minimizing variations in solar heat loading and to avoid capsule vibrations by smooth applications of forces and torques when adjusting capsule position and attitude. The experimental method and error estimates are described in Secs. IV–VI.

Several considerations favor a new measurement of G at this time. Most obvious is the desire simply to improve the determination of what is perhaps the most fundamental of all constants. The masses of the Earth and other bodies in the solar system are also necessarily unknown to the same uncertainty as G. Moreover, the stated error in G of 128 ppm may be optimistic, since three recent measurements claiming small errors differ among themselves by several hundred parts per million [1–3,6]. The Committee on Data for Science and Technology (CODATA) task group relied solely on the Luther and Towler measurements in 1986, citing unknown or inadequately evaluated systematics in the other experiments [1]. For an excellent discussion of the status of the determination of G, see Gillies [4].

More seriously, even the inverse-square law and the equivalence principle have come under scrutiny in the wake of the recent flurry of experimental activity in search of a possible "fifth force" [7–10], which in turn followed a brief period of interest in possible non-Newtonian effects at very short range [11]. Although initial reports of short-range deviations were soon discounted [11] and most of the purported fifth-force observations also can now be accounted for by extreme sensitivity to models [12–14], the recent activity has provided a reminder that verification of Newtonian gravity necessarily takes the form of upper limits on possible violations. These investigations have cast the problem of validating the inverse-square law in terms of the possible size of an additional Yukawa-type force which might remain undetected, given present experimental accuracy. The potential, including a possible non-Newtonian term, may be written as

$$U_{12}(r)=-(m_1m_2G/r)(1+\alpha e^{-r/\Lambda}) , \tag{1}$$

where α is the field-strength parameter and Λ is the characteristic interaction length. The investigations of possible short-range deviations generally followed Fujii's conjecture [11] that α is $\frac{1}{3}$ and then sought to determine upper limits on Λ. In contrast, fifth-force investigations [7–10] have treated α as a free parameter, reflecting exchanges based on baryon and lepton numbers (or possibly hypercharge), and have generally sought either to estimate both α and Λ (equivalently, m_bc^2) or to place upper limits on α, given assumed values of Λ. It is now conventional to reexpress α as the product of the presumed fifth-force "charges" and either a dimensionless coupling constant α_5 or a coupling strength g_5; specifically $\alpha=\alpha_5(q_5/\mu)_1(q_5/\mu)_2$ or $\alpha=\pm(g_5^2/4\pi)(q_5)_1(q_5)_2/(Gm_1m_2)$, where μ denotes mass in amu [15,16]. With the latter form, Eq. (1) is

$$U_{12}(r)=-m_1m_2G/r \pm(g_5^2/4\pi)(q_5)_1(q_5)_2(1/r)e^{-r/\Lambda} . \tag{1a}$$

The form of the "charge" q_5 is predicted to depend on whether the presumed mediating boson is vector or scalar [16,17]. In either case the quantities $(q_5/\mu)_i$ are expected to be of order unity for most elements (however, if the mediator is a *vector* boson, then for some elements the baryon and lepton contributions to q_5 may approximately cancel each other, depending on the value of an unknown mixing angle, θ_5).

In this paper we use the more phenomenological form Eq. (1), with its parameter α, rather than Eq. (1a), with g_5^2 (or equivalently α_5). The former equation allows a more general interpretation, which we believe is preferable for planning a long-range experiment, given the current state of rapid flux of fifth-force theories.

The present upper limit on α depends on Λ (m_bc^2) in the sense that accumulated experimental data place

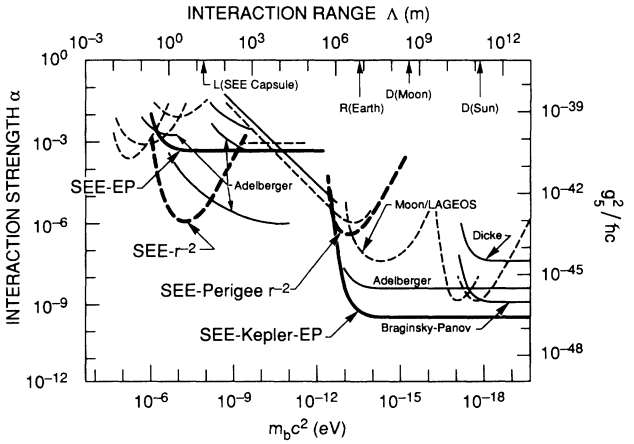

FIG. 1. Upper limit on the field-strength parameter α as a function of the interaction length Λ based on accumulated experimental data (1-σ). It is assumed that the mediator is a vector boson and the fifth-force charge is the baryon number (for variants see Ref. [16]). Dotted curves are based on tests of the inverse-square law. (This figure is adapted from de Rújula [18] and Adelberger [16].) Four new curves would be contributed by the proposed experiment: 1. SEE-r^{-2}: Test of the inverse-square law using shepherd-particle interaction. 2. SEE-Perigee-r^{-2}: Test of the inverse-square law using Earth-test-body interaction. 3. SEE-EP: Test of the equivalence principle using shepherd-particle interaction. 4. SEE-Kepler-EP: Test of the equivalence principle using Earth-test-body interaction.

stricter limits at some distances (masses) than at others [18,19]. The limits are generally much better at astronomical distances than at typical laboratory distances and are most poorly known at distances on the order of meters (masses $\sim 10^{-7}$ eV/c^2). Figure 1 illustrates the present limits on α: the four dark curves marked "SEE-r^{-2}," "SEE-EP," and "SEE-Perigee-r^{-2}," and "SEE-Kepler-EP" indicate the expected results of our proposed tests.

The interaction between the two test bodies in a SEE encounter will test both for violations of the inverse-square law and for composition-dependent differences (Eötvös' experiment), which may also be interpreted as violations of the equivalence principle. Assuming a null result, each test will place a bound on $|\alpha|$, given any assumed value of the characteristic length Λ. For $\Lambda \sim 1$ m ($m_b c^2 \sim 2\times 10^{-7}$ eV), the present upper limit on α is an uncomfortably large 10^{-3}. The interaction between the two test bodies would be most sensitive to violations of the inverse-square law if Λ is a few meters, since this is the typical separation of the test bodies; it would be capable of detecting α as small as 10^{-5} to 10^{-6} for 50 cm $< \Lambda <$ 50 m (curve "SEE-r^{-2}"). This test would place new upper limits on α if the characteristic length Λ is anywhere in the interval 30 cm $< \Lambda <$ 30 m (7×10^{-9} eV $< m_b c^2 < 7\times 10^{-7}$ eV). Moreover, for 30 m $< \Lambda <$ 1 km, this test will also provide the best limit on α inferred from the *inverse-square law* rather than the equivalence principle.

The interaction between the two test bodies would be sensitive to any composition-dependent differences in α (equivalence-principle violations) for all values of Λ *greater* than the test-body separation (curve "SEE-EP"). It would detect composition-dependent *differences* in α (not α per se) as small as 5×10^{-7} for $\Lambda > 5$ m ($m_b c^2 < 4\times 10^{-8}$ eV). The corresponding limit placed on $|\alpha|$ is about 3 orders of magnitude weaker [20] (however, a bound on α inferred from an equivalence-principle test is fairly model dependent, being sensitive to the particular assumptions about q_5 and the form of the interaction). Thus, the limit $|\Delta\alpha| < 5\times 10^{-7}$ corresponds to $|\alpha| < \sim 5\times 10^{-4}$. This is less stringent than Adelberger's bound at intermediate distances (see Fig. 1).

Completely separate tests are provided by the interaction of the test bodies with the Earth rather than with each other. The precession of perigee of the two test masses in their Earth orbits can be accurately measured if their orbits are slightly different. A test for inverse-square violation based on perigee precession would marginally improve the limits on α if $\Lambda \sim 1000$ km ($m_b c^2 \sim 2\times 10^{-13}$ eV), with a limit of 10^{-5} to 10^{-6} or less on α for 1000 km $< \Lambda <$ 100 000 km (curve "SEE-Perigee-r^{-2}"). This test is expected to be less restrictive than Adelberger's results for $\Lambda > 1000$ km or than the "Moon-LAGEOS" results for $\Lambda > 5000$ km. Nevertheless, this test is interesting as a confirmation of these earlier results.

A very sensitive test of the equivalence principle will also result from the interaction of the Earth with the test bodies, since the apparent constant GM_{Earth} as determined from Kepler's third law would reflect composition-dependent differences in α. For all values of Λ *greater* than one Earth radius ($m_b c^2 < 3\times 10^{-14}$ eV) this effect will test the equivalence principle to within 4 parts in 10^{13}; that is, $|\Delta\alpha| < 4\times 10^{-13}$ for $s > R_{\text{Earth}}$ (hence $|\alpha| < \sim 4\times 10^{-10}$; curve "SEE-Kepler-EP" in Fig. 1). Please refer to "Note added in proof" below.

For $\Lambda > 1$ astronomical unit (AU), our estimate of this bound is comparable with the results of the Dicke and Braginsky experiments [21], and for $R_{\text{Earth}} < \Lambda < 1$ AU it is comparable to Adelberger's new bound on α [16]. An intriguing new equivalence-principle proposal [22], which uses a Braginsky-Dicke pendulum [21] and employs water as the attractor, expects a bound on $\Delta\alpha$ that would be somewhat more stringent than ours at short distances. However, the bounds from our equivalence-principle tests will not be comparable with those expected from STEP (satellite test of the equivalence principle), the elegant new experiment proposed by the Stanford group [23].

Interest in the possibility of a time-varying G was initiated by Dirac's large-numbers hypothesis (LNH) [24], which suggested that the rate of change should be $\dot{G}/G \sim -(\text{age of the Universe})^{-1} \sim -7\times 10^{-11}$/yr. Several recent theories also require a changing G and make specific predictions of $\dot{G}/G$. Moreover, such a test may be one of very few ways of testing for extra dimensions [25]. The experimental situation is somewhat muddled. Various attempts to determine $\dot{G}$ by indirect means, involving imaginative analyses of such diverse phenomena as ancient eclipse records, nucleosynthesis, and binary pulsars, have yielded a puzzling collection of (1) stringent upper limits on $|\dot{G}/G|$ (as small as 1.7×10^{-13}/yr or even 5×10^{-17}/yr) and (2) various nonzero estimates of $\dot{G}/G$ (typically from -10^{-12}/yr to -10^{-10}/yr) [26]. This apparent inconsistency suggests the desirability of a *direct* measurement under *controlled* conditions. Preliminary analysis suggests that a measurement of $\dot{G}$ by Kepler's third law using the SEE satellite may be capable of discriminating among the various theories.

In short, we propose six measurements or tests with the SEE satellite: (1) a measurement of G at distances on the order of meters; (2) a test of the inverse-square law at distances on the order of meters (curve SEE-r^{-2} in Fig. 1); (3) a test of the inverse-square law at distances on the order of an Earth radius (curve SEE-Perigee-r^{-2} in Fig. 1); (4) a test of the equivalence principle at distances on the order of meters (curve SEE-EP in Fig. 1); (5) a test of the equivalence principle at distances on the order of an Earth radius (curve SEE-Kepler-EP in Fig. 1); (6) a measurement of $\dot{G}$ at distances on the order of one Earth radius.

The results of four of these tests would represent significant advances beyond current knowledge. The tests of the inverse-square law at one Earth radius (the third test) and of the equivalence principle at a few meters (the fourth test) are of interest mostly as confirmations of previous experiments with equal or better precision. (A possible seventh test, measuring $\dot{G}$ at distances on the order of meters, will be unfeasible unless distance resolution can be improved by 2 orders of magnitude.)

II. BASIC PRINCIPLES OF THE SATELLITE ENERGY EXCHANGE (SEE) METHOD

The SEE method exploits a little-known special case of the restricted three-body problem, namely, the horseshoe-orbit phenomenon. This phenomenon was predicted by Darwin in 1897 in a remarkable treatise on periodically perturbed orbits [27] but largely neglected until its application to planetary rings and the newly discovered co-orbiting satellites of Saturn in the late 1970's and early 1980's.

The principle of a SEE encounter may be understood by considering two satellites in identical circular orbits around the Earth, one behind the other. If the gravitational attraction between the satellites were zero, they would continue forever in the same circular orbit (neglecting drag, gravitational anomalies, etc.) with the same spacing. However, the mutual gravitational attraction will decrease the energy of the leader, causing it to spiral inward, and increase the energy of the trailing satellite, causing it to spiral outward, and *the two satellites may move apart.* In his 1897 paper Darwin outlined the conditions for such an apparent *repulsive* gravitational interaction, paradoxical though it may seem, and classified the various possible orbital perturbations on a small body due to a more massive co-orbiting body.

More recently Dermott and Murray [28] and Yoder *et al.* [29], among others, have applied Darwin's analysis to the shepherding of the rings of the major planets and have extended it to the gravitational interaction of satellites which have comparable masses. Dermott and Murray find that the horseshoe-orbit phenomenon can explain apparent anomalies in the orbits of the recently discovered Saturnian satellites 1980S1 and 1980S3 (hereafter simply "S1" and "S3"), which are in nearly identical circular orbits. The energy exchange results from the following relative movements of the two satellites: From the vantage point of the more massive S1, the smaller S3 appears to be moving *forward* very slowly whenever it is in a slightly *lower* (and therefore *"faster"*) orbit than S1. If S3 is approaching S1 from behind, then S3 would eventually overtake S1, but because S3 gains energy during the encounter, it rises to a higher ("slower") orbit than S1, whereupon S3 begins to fall behind. S3 continues to recede until it encounters S1 again after falling behind nearly one complete relative revolution. This time S3 of course enters the encounter at a *higher* orbit than S1, and the energy loss to S1 during this encounter sends S3 back into a lower orbit, whereupon it resumes relative prograde motion, thus completing the cycle. Darwin noted that the pattern which would be traced by the predicted motion of the smaller body relative to the larger body during such a sequence of encounters resembles the outline of a circular horseshoe [27] a term which persists in the modern literature.

Librations of the larger body must also be taken into account (see Fig. 2) if the masses of the two satellites are comparable (which is in fact the case with S1 and S3) or if extreme precision is required, as will be the case in using the SEE method to measure G and test Newtonian gravitation. In any case, it is always the leading body which loses energy in such an exchange and descends into a lower and "faster" orbit, while the trailing body gains energy in the exchange and climbs into a higher and slower orbit, and the result is the paradoxical appearance of a *repulsive gravitational interaction.* The basic reason for this phenomenon is the virial theorem: The energy exchanged during an encounter cannot be converted into kinetic energy because the average ratio of kinetic and potential energy must be $KE/PE = -\frac{1}{2}$ if the force is pure inverse-square without perturbations, which is essentially true in the proximity of a planet. Thus, any process which gradually decreases (increases) the total energy of an orbiting body by some amount will *increase (decrease)* its kinetic energy by approximately the same amount.

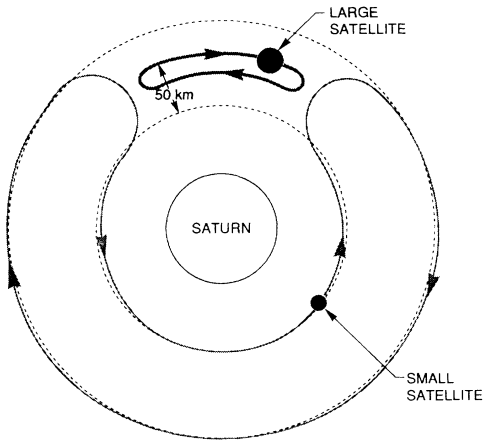

FIG. 2. Partly schematic diagram of the orbital configuration of the co-orbital satellites of Saturn, 1980S1 and 1980S3 (after Dermott and Murray [28]). Note that the satellites recede from each other after each encounter.

It should not be assumed that encounters between satellites in nearly identical orbits will necessarily result in horseshoe orbits (or other periodic perturbations). It is easy to imagine situations in which the gravitational interaction will result in either a capture, scattering, or a gravitationally bound pair. Darwin's treatise and much of the recent literature are concerned with determining the boundaries of these various cases. Among the more interesting cases are the "tadpole" orbits, which are librations about one of the Lagrange points L4 or L5 and are named for their shape [27].

III. MECHANICS OF PROPOSED SEE ENCOUNTERS

To make gravitational measurements using a horseshoe orbit, we propose to monitor the position and velocity of a "particle" very accurately as it first approaches and then recedes from a large "shepherd" mass during a satellite energy exchange (SEE). This approximates the encounter phase of a horseshoe orbit.

For illustrative purposes the mass of the particle may be taken as infinitesimal and the orbit of the shepherd may be taken as circular. The Newtonian Lagrangian of the interaction then reduces to (for a treatment of eccentric shepherd orbits, see Dermott and Murray [28])

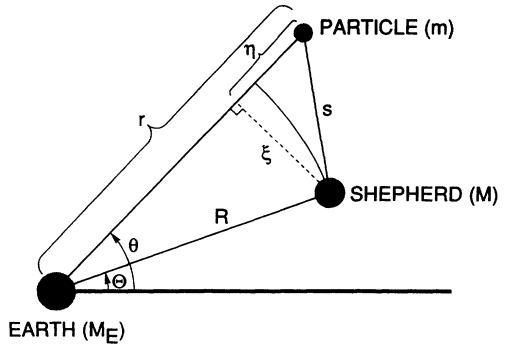

FIG. 3. Geometry of variables in SEE encounter.

$$L=\tfrac{1}{2}m(\dot{r}^2+r^2\dot{\theta}^2)+M_E mG/r+MmG/s \tag{2}$$

and therefore the equations of motion of the particle are

$$\ddot{r}-r\dot{\theta}^2=-M_E G/r^2-(MG/s^3)\eta \tag{3}$$

and

$$r\ddot{\theta}+2\dot{r}\dot{\theta}=-(MG/s^3)\xi\ , \tag{4}$$

where s is the separation of the test bodies and m, M, and M_E are the masses of the particle, the shepherd, and the Earth. The geometry is shown in Fig. 3. The rectangular coordinates (ξ,η) are defined by

$$\begin{aligned}\xi&=R\sin(\theta-\Theta)\ ,\\ \eta&=r-R\cos(\theta-\Theta)\ ,\\ s^2&=\xi^2+\eta^2=|\mathbf{r}-\mathbf{R}|^2\ .\end{aligned} \tag{5}$$

Note that Eqs. (3) and (4) reduce to the classical two-body problem if $M=0$ or $s\sim\infty$. The equations of motion of the shepherd are simply $R=$const and $\Theta=\omega_0 t$.

In the usual space paralance, ξ and η are essentially the along-track and radial components of the shepherd's position relative to the particle. The reason that the coordinate axes are based on the particle rather than the shepherd or the center of mass of the two test bodies, as might be expected, is the resulting simplicity of Eqs. (3) and (4).

Figure 4 shows our results from computer modeling of

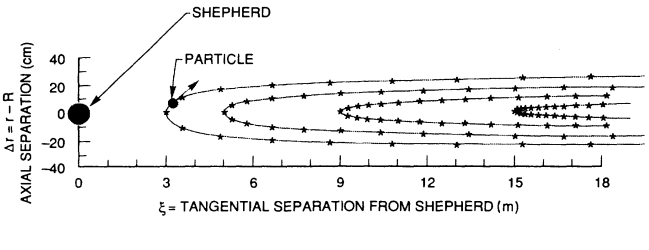

FIG. 4. Some possible trajectories of a particle of negligible mass in a SEE encounter with a 500-kg shepherd, relative to a coordinate system moving with the shepherd and rotating with its orbital motion. The particle approaches the shepherd and then recedes from it. Dots indicate 10 000-sec intervals. Note that the vertical scale is magnified $\times 5$ for clarity.

Eqs. (3) and (4) for encounters at selected distances of closest approach, s_0. In these simulations, the eccentricity of the particle orbit was chosen to be asymptotically zero as the separation of the two bodies approaches infinity. For a 500-kg shepherd, the encounter paths are very narrow: the difference in the (Earth-centered) radii of the two bodies is asymptotically $\Delta r<27.4$ cm for all $s_0>3$ m. The encounter paths are also nearly U shaped: they have about 70% of their ultimate width where $s=2s_0$. Thus, the geometry of an encounter is virtually one dimensional from the viewpoint of the shepherd.

As expected, the time required for the particle to traverse any portion of the encounter path scales essentially as $(MG)^{-1/2}$, which provides the basis for measuring G. Figure 4 shows that the duration of an encounter out to $s=20$ m is a few days for typical values of s_0. Note that for encounters of a given maximum length, the durations are longer for *intermediate* values of s_0 than for large or small s_0. Specifically, the encounter duration reaches a maximum when s_0 is $\sim 61\%$ of the maximum separation, a fact with important implications for accuracy.

The encounter duration is strongly independent of the gravitational attraction of the Earth, and it varies only slightly with the orbital period of the shepherd: Our modeling shows that a hypothetical *eightfold* increase in the mass of the Earth (holding G and the shepherd's period constant) would change the duration for a 20-m encounter by only a few parts in 10^6. Similarly, a 1% change in the period of the shepherd (holding G and the Earth's mass constant) would change the encounter duration by a few parts in 10^5. Clearly, these effects will have negligible impact on the experimental error, since the mass of the Earth is known to <2 parts in 10^4, and the orbital period will be known to <1 part in 10^8. Note the symmetry in the radial component of position, in agreement with results of Dermott and Murray [28]. We find that the symmetry is within $\sim 3\times 10^{-9}$ m for $s_0>3$ m (we plot Δr rather than η because the curvature of the orbit spoils the symmetry in η).

Since G may be determined from a *portion* of the encounter path, any deviation from the inverse-square law would manifest itself as an apparent variation of G with s. This is the basis for testing the inverse-square law at intermediate distances. For a simple two-point comparison at distances $s\sim s_1$ and $s\sim s_2$, the upper bound placed on α by a null result would be (after de Rújula [18])

$$\begin{aligned}|\alpha|<\varepsilon[&(1+s_1/\Lambda)\exp(-s_1/\Lambda)\\ &-(1+s_2/\Lambda)\exp(-s_2/\Lambda)]^{-1}\ ,\end{aligned} \tag{6}$$

where ε is the sensitivity with which MG can be measured on each portion of the encounter path. For two given separations s_1 and s_2, the maximum of the bracketed quantity in Eq. (6) occurs at $\Lambda=0.5(s_1-s_2)/\ln(s_2/s_1)$, and the maximum is 0.830 if we let $s_2/s_1=8$. (It is of order unity provided s_2 is at least several times s_1). Letting $s_1=2$ m and $s_2=16$ m and assuming $\varepsilon=10^{-6}$, we find that the smallest upper bound on α occurs at $\Lambda\sim 3.36$ m and is $|\alpha|<1.2\times 10^{-6}$, as reflected in Fig. 1 by the curve SEE-r^{-2}.

In contrast with inverse-square law tests, a null result for an equivalence-principle test would place an upper limit on the *difference* $\Delta\alpha$ between values of α for two different particle compositions. Comparing the force [found by differentiating Eq. (1)] of the shepherd on two particles of different composition at the same separation s provides a test of any difference in their coupling to the shepherd:

$$\Delta\alpha=\alpha_1-\alpha_2=\varepsilon[(1+s/\Lambda)\exp(-s/\Lambda)]^{-1} . \quad (7)$$

The resulting limit is virtually constant for all values of the characteristic interaction length *exceeding* the typical separation of the test bodies (curve SEE-EP in Fig. 1). This constant behavior reflects the fact that the Yukawa potential [Eq. (1)] is asymptotically $U(r)=-(MG/r)(1+\alpha)$ when $\Lambda\gg r$.

If the particle approaches the shepherd along a path that does not correspond to an asymptotically zero-eccentricity orbit, and if the orbital conditions also result in a SEE encounter with the shepherd, then the particle's motion during the SEE encounter is roughly a superposition of (1) the motion of a particle with asymptotically zero eccentricity and (2) the oscillating difference $(\Delta r(t),\Delta\theta(t))$ between unperturbed elliptical and circular orbits. The path resembles a cycloid but with oblong loops, as shown in Fig. 5. It is typically prolate near closest approach and may be either prolate or curtate for large s, depending on the specifics of the encounter.

These cycloidal oscillations $(\Delta r(t),\Delta\theta(t))$ are the basis for testing the inverse-square law at characteristic distances Λ on the order of one Earth radius. This may be done straightforwardly by comparing the apsidal and anomalistic periods of the shepherd. The principle of this method may be seen by treating the shepherd's motion as due to a central force including a small (central) perturbation. It can be shown that in this case the orbital equation $u=u(\theta)$, where $u=1/r$, may be expressed as a cosine Fourier series in $\gamma\theta$:

$$u(\theta)=u_0+A_1\cos\gamma\theta+A_2\cos2\gamma\theta+\cdots , \quad (8)$$

where the parameter γ, which describes the perigee precession rate, may be measured as the ratio of the anomalistic (360° revolution) and apsidal (perigee-to-perigee) periods:

$$\gamma=T_{\text{anon}}/T_{\text{aps}} \quad (9)$$

and is related to the perturbing potential, to lowest order, by

$$\gamma=\sqrt{(1-dh/du)|_{u=1/a}} , \quad (10)$$

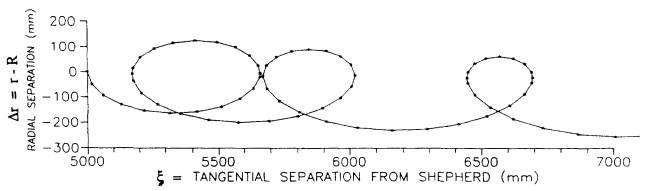

FIG. 5. A particle trajectory for nonzero asymptotic eccentricity. The cycloidal loops of the particle indicate its apsidal period. Vertical scale *not* exaggerated, unlike Fig. 4.

where h is the right side of the general orbital differential equation for the central-force problem [30]:

$$d^2u/d\theta^2+u=-(1/u^2)(mL^2)f(1/u)=h(u) . \quad (11)$$

For the Newtonian potential, $h(u)$ is constant. With a Yukawa perturbation (Eq. 1), we have

$$dh/du|_{u=1/a}=\alpha[(1/u\Lambda)^2\exp(-1/u\Lambda)]_{u=1/a}=\alpha[(a/\Lambda)^2\exp(-a/\Lambda)] . \quad (12)$$

Thus, given any assumed value of Λ, a measurement of the perigee precession rate [Eq. (9)] places an upper bound on α [Eqs. (10) and (12)]; namely,

$$|\alpha|<\{1-(T_{\text{anon}}/T_{\text{aps}})^2\}[(a/\Lambda)^2\exp(-a/\Lambda)]^{-1} . \quad (13)$$

The quantity in square brackets reaches its maximum (0.541) when $a/\Lambda=2$. Thus, the most sensitive value of Λ is $\Lambda\sim3900$ km, if the satellite's altitude is chosen ~1500 km (see below). It would not be possible to measure the apsidal period of an isolated satellite in a low-eccentricity orbit (such as the shepherd alone) to sufficient accuracy. However, with *two* bodies in slightly different orbits this is possible, since the cycloidal variation of their relative position is closely related to their apsidal periods. It must be emphasized that this could be done essentially by an empirical curve-fitting process and *without knowledge of the gravitational fields of the shepherd and the capsule.*

During a typical SEE encounter, the number of orbital revolutions (and, hence, of cycloids) is 30 to 40 (assuming a 2-hour orbital period). The accuracy with which the cycloidal period can be determined will be limited chiefly by the distance accuracy χ and the relative velocities of the particles. The oscillatory contribution to the relative position (ξ,η) will be nearly simple harmonic motion. Hence the peak velocity contribution from the oscillation will be $(-\omega\xi_{\max},\omega\eta_{\max})$. The largest feasible cycloid to fit inside the capsule (see below) is ~80 cm long and ~40 cm high, for which the maximum oscillatory velocities are $\sim(350, 175)$ μm/sec. Assuming the horizontal distance accuracy χ is $\chi=0.25$ μm, it follows that the apsidal period T may be measured to $\sim\chi/(\omega\xi_{\max})\sim7.1\times10^{-3}$ sec $\sim1.0\times10^{-7}$ T. Thus γ can be determined to within 1 part in 10^7 [Eq. (8)], dh/du can be determined within $\pm2\times10^{-7}$ [Eq. (10)], and α may be determined within dh/du $[(a/\Lambda)^2\exp(-a/\Lambda)]^{-1}$ [Eq. (12)]. When Λ is most sensitive, the quantity in the brackets is 0.541, and therefore the bound on α is $|\alpha|<3.7\times10^{-7}$, which is reflected in Fig. 1 by the curve "SEE-Perigee-r^{-2}."

Nonspherical terms in the Earth's potential cause perigee precession at a rate 2 or 3 orders of magnitude larger than the contribution from the Yukawa perturbation if $|\alpha|\sim10^{-6}$. It will nevertheless be possible to separate any Yukawa contribution from the much larger total precession rate because the contribution due to the Earth's potential is known to better than 1 part in 10^5. Perigee precession may not be the only way to infer α from the cycloids. It will be possible to determine the relative ve-

locities of the shepherd and the particle to within a few parts in 10^{15} of their orbital velocity. This may also provide an extremely sensitive test of Kepler's second law. Note that the high-precision information in this case is in tangential (rather than radial) velocity and position, which is essentially the particle-shepherd range as a function of time.

The relative motion of the shepherd and particle also provides a sensitive test of the equivalence principle (regardless of the asymptotic eccentricity of the particle): a measurement of the difference in the apparent value of GM_{Earth} as experienced by the two bodies, and hence of α, may be obtained from Kepler's third law, treating the small shepherd-particle interaction as a perturbation. If we ignore the shepherd-particle interaction and use Eq. (1) to describe the interaction of the *Earth* with either test body, then Kepler's third law becomes

$$4\pi^2 r^3/(GM_{\text{Earth}}T^2)=1+\alpha[(1+r/\Lambda)\exp(-r/\Lambda)] . \tag{14}$$

Any composition-dependent difference $\Delta\alpha$ between the two test bodies would manifest itself as a slight difference in their orbital radii if they had identical periods. From Eq. (14), this difference would be

$$\Delta\alpha=3\Delta r/r\{4\pi^2 r^3/(GM_{\text{Earth}}T^2)\}[(1+r/\Lambda)\exp(-r/\Lambda)]^{-1} . \tag{15}$$

The error in Δr will be about 1 μm, so $\Delta r/r$ will be known to $\sim 1.3\times 10^{-13}$ (the accuracy of $\Delta\alpha$ is not limited by the error in period, since $\Delta T/T$ is known to $<10^{-14}$). The resulting bound on α is shown by curve SEE-Kepler-EP in Fig. 1. Here we assume again $|\Delta\alpha|\sim 10^{-3}|\alpha|$. Note that the quantity in square brackets in Eq. (15) captures nearly all the dependence of $\Delta\alpha$ on r and Λ, since the quantity in curly brackets is virtually unity for all r/Λ, as seen from Eq. (14). Equations (6), (7), (13), and (15) all use the assumption that the attracting mass (the shepherd or the earth) is concentrated at a point. This assumption understates any Yukawa force and therefore results in a conservative statement of the bounds on α. At intermediate distances this is of little consequence (the "SEE-r^{-2}" and "SEE-EP" curves in Fig. 1), but at distances on the order of one Earth radius the left side of the true α-vs-Λ curve is less steep than indicated by the "SEE-Perigee-r^{-2}" and "SEE-Kepler-EP" curves in Fig. 1.

Finally, if the orbits of the particle and shepherd are not mutually coplanar, an additional oscillation results which obviously is roughly horizontal, across track, and periodic with the satellite.

Given the available precision, a number of systematic effects will be large enough that it will be necessary to take account of them. For example, differential accelerations of the two test bodies in the Earth's nonspherical potential field must be accounted for. As a second example, when the satellite is approaching or receding from the Moon, the two test bodies will experience a slight difference in acceleration, which alternates in sign with essentially the period of the satellite. This effect will introduce a small oscillation in the separation of the test bodies with amplitude ~ 5 μm if the test bodies are 10 m apart. Although these effects and the cycloidal oscillations are of similar magnitude, they will be easy to separate by differences in phase and amplitude. For example, the phase of the cycloids may be chosen at will for each encounter, and the differential acceleration due to the Moon will essentially vanish every two weeks if the satellite's orbit is nearly polar.

These results emphasize two points: The test bodies are fundamentally in *Earth* orbits, which are only slightly perturbed by each other, and the SEE encounter is a remarkably sensitive way of measuring perturbations.

IV. EXPERIMENTAL CONSIDERATIONS

The interacting masses need to be enclosed inside a conducting shell, called the "capsule," to protect them from atmospheric drag, radiation pressure from both the Sun and the Earth, and electric and magnetic fields, all of which would be at least comparable to the gravitational attraction between the masses. The capsule would be equipped with a system of optical lasers and interferometric sensors to monitor its own size and shape and the positions of the shepherd and particle. The proposed configuration is shown in Fig. 6 and Table I below.

The shepherd "floats" near the axis of the cylinder at various predetermined positions between the middle and one end of the capsule. The particle is "launched" from the opposite end with the necessary speed and direction to effect preplanned SEE encounters with the shepherd. A disturbance-compensation system maneuvers the capsule to prevent it from touching either body and essentially follows the orbit of the shepherd. Such systems have been in use since 1971, when the original "DISCOS" system was deployed on the Transit TRIAD

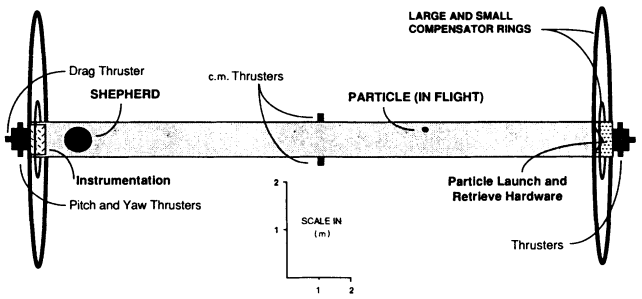

FIG. 6. Diagram of the capsule containing the "shepherd," "particle," and instrumention. The large rings on the ends cancel the internal gravitational field of the cylinder itself and of the instrumentation (vertical scale magnified $\times 1.5$ for clarity).

TABLE I. Size and composition of components.

	Mass	Composition	Dimensions
Shepherd	500 kg	Heavy metal	~40 cm diameter
Particle	100 g	Various	~2 cm diameter
Capsule cylinder	800 kg	Metal or composite	~20 m long×1 m diam
Compensator ring a	~200 kg ea	Stainless steel	~4 m radius
Compensator ring b	~75 kg ea	Stainless steel	~1 m radius
Instrumentation	~20 kg	Mixed	~0.2 cu meters total
Thrusters and fuel	~50 kg	Mixed	NA

satellite [31,32]. Fine control of attitude would be accomplished by torques from the Earth's magnetic field on small currents in fixed external coils, such as Ithaco's "Torqrods™."

The axis of the capsule cylinder is kept essentially "horizontal" and parallel to the orbital velocities of the two bodies throughout the encounter, thus enclosing the long narrow *U*-shaped SEE encounter paths. The distance s of the particle from the shepherd would typically be between 8 and 16 m at the start and conclusion of each encounter, while the distance at closest approach s_0 could be chosen anywhere from about 2 m up to 15 m.

The gravitational field due to an infinite uniform cylinder is zero internally, and for a long but finite cylinder such as the proposed capsule, the field is small except near the ends. We have shown that compensator rings, such as those shown in Fig. 6 on the ends of the cylinder, can virtually neutralize these end effects over most of the cylinder volume [33]. Throughout the central 16 meters of the cylinder, the total field of the capsule (cylinder, rings, instrumentation, and fuel) can be made less than 1% of the field due to the shepherd at a distance of 10 m. The optimum sizes of the compensator rings depend on the masses and locations of the instrumentation and fuel. We have also developed methods to calculate the required mass distribution on the surface of a closed right circular cylinder which will make it a gravitational analogue of the Faraday cage, resulting in vanishing internal field. Related work has been reported by other investigators [34].

The shepherd would be made of dense, homogeneous metal and would have nearly zero magnetic susceptibility. Particles would be made of various materials to test the possibility of composition-dependent effects. The mass of the shepherd is chosen large enough that the durations of 20-m encounters will be on the order of a few days and small enough that the *U*-shaped encounter paths will be narrow enough to fit easily into the cylinder. The mass of the particle is chosen to be small enough for ease of handling but large enough that the radiation-pressure force from the tracking lasers will be negligible compared to the gravitational force due to the shepherd.

The shepherd and particles might be spherical, but various considerations argue for alternative shapes. For example, cylinders are attractive candidates for the "large" mass in *G* experiments because of fabrication accuracy [35]. Moreover, a Cook-Marussi arrangement of stacked cylinders has vanishing nonspherical moments to high order [36], thus essentially combining the fabrication accuracy of cylinders with the ideal symmetry of a sphere. The shepherd and the particle may have either corner-cube reflectors or reflective coatings to reflect the tracking laser beams. Alternatively, the particle itself may be in the shape of an open octant corner reflector.

The tracking laser beams should have very low power (~0.01 μW) and be arranged as opposing pairs so that their radiation-pressure force on the particle will be small compared to the gravitational force of the shepherd. Use of such low power may necessitate phaselock detection of the photodetector signal. This would allow reducing the signal bandwidth to the order of 1 Hz, which will be low enough to provide adequate S/N ratio for this low beam power. A 1-Hz bandwidth in signal tracking should be more than enough to follow the dynamics of the test particle. Such a narrow bandwidth will impose a capture phase, involving a sweep-and-lock search. Submillimeter microwave methods are also highly developed now and should be considered [37]. A supplemental system for coarse ambiguity resolution is also planned to add redundancy to the distance measurements and eliminate gross errors; candidate methodologies include video, photogrammetry, and shadow detection.

The motion of the particle at the beginning and end of each encounter might be controlled simply by mechanical devices. Alternatively, eddy currents induced by coils at various locations in the capsule could be used to steer the particle into the desired orbits [38]. Short milliamp pulses at the end of an encounter would be sufficient to stop the particle and drop it into a lower orbit, thus initiating another encounter. The spins of both test bodies could be controlled by the torques from the tracking lasers.

The choice of orbital characteristics is very important. Chief among the considerations which will determine it are the altitude should be high to minimize drag; the altitude should be low to minimize high-energy particle flux from the Van Allen belts which may cause spurious electronic effects and component degradation; the orbit should be in continuous sunlight, both to minimize capsule temperature variation and to avoid "jerks" from discontinuities in solar radiation pressure when entering or leaving the earth's shadow; and, moreover, the orbital plane may need to be *very nearly normal* to the Earth-Sun line in order to further reduce temperature variation. This will be a consideration only if thermal distortion of the capsule is found to vary significantly as a function of the direction of the incident solar radiation.

These requirements conflict to some extent, so some

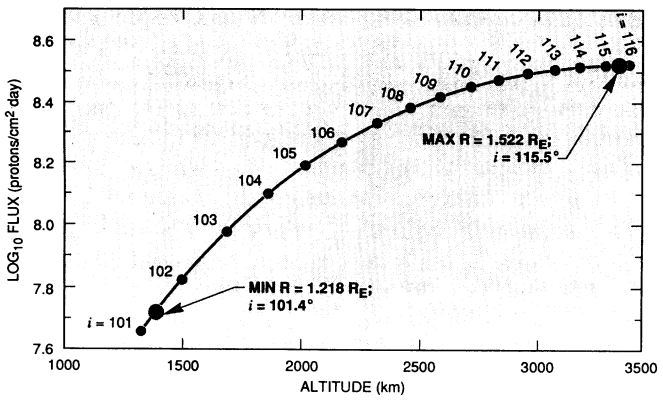

FIG. 7. Circular-orbit integrated flux (COIF) of high energy (>34 MeV) protons for continuous-sunlight orbits. To be in continuous sunlight, orbits must have altitudes between 1390 and 3330 km and inclinations between 101.4° and 115.5°. The 3330-km orbit has about six times the high-energy flux of the 1390-km orbit (from Eq. (16), including Eq. (17), and Fig. 9 of Appendix II of Hess [41]).

tradeoffs will be necessary. It is fairly easy to satisfy the requirement for continuous sunlight, by using a "sun-synchronous" orbit which has its nodes approximately on the terminator and is at a suitable altitude. The oblateness of the Earth causes the nodes to precess at a rate which depends principally on the inclination and altitude of the orbit [39]. It is possible to make the nodes precess 360°/yr ($\dot{\Omega}\sim 0.9855$°/day), which is the Sun-synchronous condition, by a suitable choice of the relation between the orbital radius R and the inclination i. For a circular orbit the relation for Sun synchronicity is

$$\cos i = kR^{3.5} , \tag{16}$$

where $k=[\frac{3}{2}J_{20}\sqrt{(GM_E/R_{E^3})}/\dot{\Omega}]^{-1}\sim -0.098\,91$ if R is in units of Earth radii. For the orbit to be in continuous sunlight, a further necessary condition is

$$R\cos\Psi > 1 , \tag{17}$$

where Ψ is the angle of incidence of the Earth-Sun line on the orbital plane. This inequality can be satisfied for Sun-synchronous orbits only with values of R in the range $1.218<R<1.522$. That is, the permissible altitudes for continuous-sunlight orbits are between $\sim$1390 and $\sim$3330 km (the radius of the Earth is taken as 6378 km). The respective inclinations from Eq. (16), are $i\sim 101.4$° and $i\sim 115.5$° [40]

Figure 7 shows the high-energy proton flux for circular orbits at all permissible continuous-sunlight altitudes. It shows that the circular orbit integrated flux (COIF) of high-energy (>34 MeV) protons varies from $\sim 5.2\times 10^7$/cm^2 day for the lowest continuous-sunlight orbit (1390 km altitude, 101.4° inclination) to $\sim 3.3\times 10^8$/cm^2 day for the highest continuous-sunlight orbit (3330 km altitude, 115.5° inclination). These fluxes are well below the maximum possible proton COIF which a satellite can experience, namely, $\sim 1.6\times 10^9$/cm^2 day, which occurs in an equatorial orbit ($i=0$) at 3400 km altitude [41].

In the low end of the permissible altitude range, the inclinations of continuous-sunlight orbits are nearly polar, which ipso facto would keep the orbit roughly normal to the Earth-Sun line year round. Moreover, for six months of the year this requirement may be met remarkably well. For example, the inclination of a 1500-km orbit is 102.0°, which differs only 12° from polar. This is fortuitously about half the obliquity of the ecliptic ($\sim$23.5°). It follows that $\Psi\leq 12$° for six months: clearly $\Psi\sim 12.0$° at the equinoxes, and $\Psi\sim 11.5$° (23.5−12.0) at one solstice (say, summer), and Ψ passes through zero about April 22 and August 22. At the other solstice $\Psi\sim 35.5$° (23.5+12.0). The solar radiation impinging on the capsule will vary approximately as the sine of the angle between its axis and the Earth-Sun line. Therefore, if the capsule axis is oriented along its orbital velocity vector, the incident solar radiation then will oscillate with a period half the orbital period and with amplitude $\sim 0.5(1-\cos\Psi)$. Thus, for six months this amplitude would be less than 1.1% for a 1500-km continuous-sunlight orbit, while the maximum amplitude, which of course occurs at the other solstice, would be $\sim$9.3%.

To keep the capsule oriented with its axis horizontal and in the orbital plane, it will be necessary to continually apply small torques with the external coils. In essence, the rotational angular momentum must be kept nearly aligned with the orbital angular momentum, which is continually changing due to the torque from the Earth's obliquity.

Note that the along-track components of solar radiation force will generally be small in a continuous-sunlight orbit (because the capsule's orbital velocity is roughly perpendicular to the incoming solar radiation), and it will average to nearly zero over one orbit. The main result of the Sun's radiation pressure is to displace the capsule's orbital plane about 8 cm from the Earth's center of mass. Moreover, the along-track component of the force due to Earth radiation is negligible, since the orbital track roughly coincides with the terminator except at high latitudes.

A completely different choice of orbital parameters may be preferable if analysis shows that spurious electronic effects from high-energy Van Allen radiation are a very serious problem at the low detection levels needed for the tracking lasers, but that fluctuations in thermal distortion of the capsule are not a problem. This would mean going either much lower or much higher to avoid Van Allen radiation: To reduce the flux of high-energy protons to $<5\times 10^6$/cm^2 day (one-tenth the COIF in a 1390-km continuous-sunlight orbit), the altitude must be either <700 km ($R=1.11$) or >10 000 km ($R=2.57$), assuming a polar orbit [41]. However, continuous-sunlight orbits are not possible below 1390 km or over 3330 km, as shown above [moreover, even Sun-synchronous orbits are impossible at altitudes over 5975 km ($R=1.937$), as seen from Eq. (16)]. Therefore, at 700 or 10 000 km altitude, the solar radiation incident on the capsule would vary substantially during each orbital revolution due to eclipsing and to variation of the capsule's orientation toward the Sun. The nature of this variation naturally divides the year into four "seasons": during

two opposite "seasons" the satellite is eclipsing every orbit; this is when the Sun is close to the plane of the satellite's orbit. In the other two "seasons" the satellite is in continuous sunlight, but the radiation pressure oscillates twice per orbital revolution with amplitude $\sim 0.5(1-\cos\Psi)$. Near the middle of each of these seasons Ψ goes through zero, and it is small in the vicinity of the null (clearly, $\Psi \sim n^0$, where n is the number of days before or after the null).

Several general considerations apply to virtually any orbit which might be considered. The vacuum is so hard that drag on the test bodies *within* the capsule will be negligible at their relative speeds (on the order of 0.1 mm/sec). The mean time between molecular collisions within the capsule would be on the order of an hour at altitude ~ 2000 km [42,43]. Drag is so low at these altitudes that thruster life is no issue. In fact, for a spherical satellite at orbital velocities, drag is about equal to radiation pressure at 500 km altitude [44], and it is 3 orders of magnitude less at 1500 km altitude [43]. Because this ratio is so large, drag on the capsule can be overcome simply by adjusting its *attitude* so that it "sails" on solar radiation pressure. A yaw of about 10^{-4} radian will be sufficient to completely offset the average circular-orbit integrated drag on our capsule (nose deflected ~ 1 mm sunward from the ortbital plane; tail deflected ~ 1 mm away from the Sun). Note, however, that drag varies an order of magnitude due to solar-cycle variations [43], and therefore the required yaw must be adjusted empirically in orbit.

The motivation for "sailing" is not to conserve thruster fuel, but rather to produce a smooth, jerk-free capsule motion [although fringe measurements should not in principle be vitiated by firing the DISCOS thrusters, this would probably introduce very-low-frequency (<1 Hz) oscillations to the capsule, and prudence dictates that SEE encounters should be as "clean" as possible]. Moreover, the attitude-control coils can trim the capsule orientation to produce the required sail thrust with essentially no jerking. Finally, the thrust should be calculated on a whole-orbit-average basis, which requires a "smart" DISCOS brain capable of planning several orbits in advance, rather than a conventional servo-feedback system.

V. SOURCES OF ERROR

At the scale of this experiment, time resolution is effectively unlimited and will therefore contribute negligible error.

Distance resolution of ~ 0.05 optical wavelength, or 0.03 μm, is expected ($\lambda \sim 633$ nm). For a 16-m encounter, this gives a distance resolution of 2 parts in 10^9. Optical heterodyning systems with $\frac{1}{128}$ fringe (and hence distance resolution of $\frac{1}{256}$ wavelength or ~ 0.002 μm) are now commercially available [45], but we have assumed an order of magnitude derating because of our stringent requirement for low tracking-laser power. Moreover, to achieve our assumed resolution (0.03 μm) we would add phaselock detection capability.

Conventional wisdom might suggest that the error in measuring the separation at closest approach s_0 would limit the accuracy with which G can be determined. However, a salient and fortuitous aspect of the SEE method is that s_0 is a noncritical parameter. This is because an extremum (maximum) occurs in the encounter duration as a function of s_0, holding the maximum separation constant. The extremum occurs when s_0 is $\sim 61\%$ of the maximum separation during the encounter (provided the asymptotic eccentricity is small). The consequence of this extremum is that the separation measurements are noncritical when s is in the immediate vicinity of s_0. In fact, an unthinkable error of a *millimeter* in s_0 would affect a determination of G by only a few parts in 10^8.

Possible sources of systematic error which must be evaluated include interference-fringe counting ambiguities, shepherd mass, shepherd mass inhomogeneities, shepherd fabrication errors, capsule warping, mass accounting of the capsule (including instrumentation, insulation, fuel, etc.), micrometeorite impacts on the capsule, laser radiation pressure on the particle, capsule orientation, and optical-path errors related to the positions of reflectors attached to the test bodies and the capsule. Several possible electromagnetic error sources must also be evaluated, including the magnetic part of the Lorentz force and Coulomb interaction of the test bodies in the event that they acquire minute charges from ionization by cosmic radiation or the tracking lasers, magnetic dipole-dipole interaction of the two test bodies, and magnetic dipole interaction with the external magnetic field.

Ambiguities in fringes are unlikely to occur, due to the use of multiple tracking lasers beaming from different directions and angles. Moreover, breaks in the fringe count would have little consequence, because it is not necessary to have unbroken data along the entire encounter path. Finally it is likely that data-reduction methods incorporating the dynamic relations (vis-à-vis strictly kinematics) can reconstruct a broken encounter with high precision.

The mass of the particle need not be very accurately known because it is small compared to the shepherd mass and essentially cancels out of the calculations.

The mass of the shepherd can be measured to 3 parts in 10^7 by the large-mass comparator of the Physikalisch-Technische Bundesanstalt (PTB) in Braunschweig [46]. This will probably be the largest error in the determination of G (although it of course will have no effect on the tests of the inverse-square law, the equivalence principle, or $\dot{G}/G$).

The accuracy of the SEE method may focus attention on the problem of defining (or realizing) the kilogram. It is one of only two physical standards still based on material objects rather than atomic properties. Moreover, mass comparisons, including the recent PTB work, are made *in air,* and are therefore subject to uncertainties from buoyancy, surface deposits, and unexplained sources [46]. Our experiment will be performed in vacuo (like all determinations of G since Braun's work at the turn of the century [47,48]) and are therefore also subject to outgassing uncertainties [49]. Such matters have been largely moot until now, however worrisome they may have been to metrologists, since all previous macroscopic experiments that relied on mass were limited by errors

other than mass determination. SEE changes all that.

In laboratory-scale determinations of G, mass-distribution anomalies in the "large" mass are generally an important component of the error budget [50], because the extreme weakness of the gravitational force requires that the test bodies be very close together. The SEE method largely obviates this problem through the large separation of the test bodies. To show this, consider a worst-case assumption that relative density anomalies of $\pm 1 \times 10^{-5}$ occur [50] in the shepherd in two opposite spherical regions of 10-cm radius (half the shepherd's radius). The result is a mass dipole of ± 0.6 g separated by 20 cm. In the same vein, a worst-case assumption for shepherd fabrication errors of a Cook-Marussi stack might be that the cylinders at opposite poles of the stack differ in length by 2 μm, which would result in a mass dipole of ± 0.3 g separated by 40 cm. The proportional change in the gravitational force of the shepherd due to a mass-anomaly dipole is $2(\delta M/M) \times (d/r)$ on the axis of the dipole, where d is the separation of the dipole elements. Thus the proportional change in the force due to either of the worst-case assumptions above would be 5×10^{-7} at 1 m, or $\sim 1 \times 10^{-7}$ at the larger separations which are typical of SEE encounters.

Moreover, with the SEE method these moments can be measured *in situ* through a series of very close encounters (< 2 m) as the shepherd assumes various orientations to the encounter path. This is quite analogous to determination of the Earth's potential field through satellite geodesy, and it will allow fine-tuning of the shepherd's field at the larger separations which are typical of SEE encounters. At these larger separations, the residual uncertainties in the moments will contribute errors of less than 1×10^{-8} to the gravitational field of the shepherd.

By similar means the gravitational field of the capsule (cylinder, compensator rings, instrumentation, and fuel) will also be gradually mapped by the cumulative data from all SEE encounters. Nominal masses and mass distributions will of course be known to high precision *a priori*, and a Fourier-Bessel series may be used to represent departures from nominal. Thus, mapping the field of the capsule consists of determining the expansion coefficients. Available distance and time resolution suggest that mass departures of ~ 0.01 g can be identified *in situ*, thus reducing the field uncertainties to the same order of magnitude as the uncertainty due to mass anomalies of the shepherd. Note that the objective of this procedure is only to find the mass *distribution* of the capsule; the mass itself essentially cancels out of the error analysis because the capsule is configured to have nearly zero internal field. Note finally that a necessary condition for this mapping is that the shepherd be located serially at several widely spaced positions in the capsule, which will make it possible to separate the effects of shepherd mass anomalies and capsule mass departures.

Micrometeorite impacts are not expected to be a problem. The impulse from a large meteorite, 1 mm diameter (a "shooting star"), would alter the capsule velocity about 100 μm/sec (assuming density of iron and relative velocity at impact of 50 km/sec), which in turn would alter the capsule orbit about 20 cm. Meteorites of this size strike a square-meter area at intervals of 120 million years [51]. At the other extreme, very small meteorites, which cause capsule acceleration fluctuations some 7 orders of magnitude below those due to solar radiation pressure, will strike the capsule at intervals of ~ 100 sec [44]. In any case the impacts will impart impulses only to the *capsule*, not the test bodies. The impulses should not upset the tracking system because the step functions to the capsule motion will be in velocity, not position. In short, micrometeorites can be neglected, even during heavy meteor showers such as Perseids and Geminids.

Thermal effects, especially capsule warping due to differential solar heating, must be kept to a minimum. The main concern is transients in the mass distribution of the capsule if these transients distort it into a varying "banana" shape. A sizable constant warp or even a small well-behaved periodic warp is of little concern. The capsule will be three-axis stabilized, with one side always facing the Sun, more or less. If the chosen orbit is a low-altitude continuous-sunlight orbit, the amplitude of the oscillation of incident solar radiation will be $< 1\%$ for six months and will peak at $\sim 10\%$ at the "other" solstice, as shown above. It follows from the Stefan-Boltzmann law that, without insulation, the capsule temperature would oscillate $< 0.25\%$ (0.5 K if the capsule temperature is ~ 200 K) during the favorable six months and ten times as much at the "other solstice" (assumes that thermal time constants are short compared to the orbital period). Insulation can reduce this oscillation at least an order of magnitude [52]. If the linear coefficient of thermal expansion is 1×10^{-6}, then the length of the capsule will therefore oscillate less than 1×10^{-6} m (two optical wavelengths) twice per orbit during the favorable six months. Insulation is also expected to reduce the front-back temperature difference of the capsule to a few degrees and its fluctuation to $\ll 0.1$ degree [52].

The above discussion assumes that the capsule axis is kept essentially parallel to its orbital velocity (that is, it is tumbled once per orbit about an axis parallel to its *orbital angular momentum*) in order to accommodate the long narrow SEE encounter paths. An alternative strategy would be to use this configuration only during the "favorable" six months, and to tumble the capsule about an axis parallel to the *Earth-Sun* line during the "unfavorable" six months, keeping the capsule axis perpendicular to this line. Although this strategy would entail the loss of some experimental time, it would achieve better year-round thermal stability by avoiding cooling during the unfavorable six months (when the daily average of incident solar radiation would fall significantly due to the $\cos\Psi$ term if the capsule were tumbled about its orbital angular momentum).

Sheathing the cylinder in radiation barriers is probably the only practical way to provide the necessary insulation. Radiation barriers are 2 orders of magnitude more effective than conduction barriers in a convection-free environment [52]. However, conventional "multilayer" insulation (silvered vinyl interleaved with bridal cloth) is not acceptable because the mass distribution must be known to high precision. Using a random-walk treat-

ment of bulging and flexing in a conventional multilayer insulation blanket, we estimate that this movement might degrade precision in the G measurement to worse than 1 ppm (assuming the blanket has a total mass of 12 kg and its subject to irregular $\sim\pm 1$ mm radial movements with a coherence width of ~ 10 cm). It should be practical to construct a semirigid barrier system consisting of a number of large thin reflective sheets which form a sleeve around the cylinder and are spaced very precisely with respect to it. Each sheet would be tied rigidly at one point but allowed to slide a small amount elsewhere as it expands and contracts independently of the cylinder.

Radiation pressure from a tracking-laser beam of power P results in a force of $2P/c$ on the particle, assuming total reflection. For an 0.01-microwatt beam this is 6.7×10^{-17} N, and, for a 100-g particle, this force is 2×10^{-6} times the gravitational force of the shepherd at a distance of 10 m. It will be necessary to have on-board capability for periodic calibration of the photodetectors and/or tracking lasers. If this can be done to within a few percent, the resulting error in G will be less than 1 part in 10^7. Moreover, the force itself can be minimized by using pairs of beams from approximately opposite directions for monitoring the particle position, so that their pressures nearly cancel.

For most of our experiments, capsule orientation can be determined satisfactorily by Sun and horizon sensors. Horizon sensors are accurate to ~ 1 milliradian on an instantaneous basis and ~ 0.1 milliradian on a full-orbit integrated basis with gyroscopic interpolation [53], while Sun sensors can be as accurate as 0.024 milliradian (5 arcsec) on an instantaneous basis [54]. Star-sighting methods will probably be necessary for the equivalence-principle test based on the interaction of the Earth with the test bodies [Eq. (15)]. In order to compare the orbital radii of the two test bodies to within 1 μm, this test requires *post facto* pitch determination within ~ 0.1 microradian (0.02 arcsec). This requirement is an order of magnitude less stringent than the HIPPARCOS design parameters [55]. Note, finally, that capsule orientation need not be *controlled* to the same accuracy to which it must be *known*.

Optical path errors may result from small movements (say, <1 μm) in the elements used to project, reflect, and detect the tracking-laser beams. For example, the nominal positions of the reflectors on the test bodies will not be exact. Fitting methods, mostly prelaunch in a laboratory setting, would be used to locate them to high accuracy. However, thermal transients in the shepherd or the particles, if any, would cause distortion. The eddy currents used to steer the particle may produce significant heating. The cooling characteristics of the shepherd also bear close investigation.

Electromagnetic effects are expected to be negligible. The surrounding capsule, being a good conductor, provides a high degree of protection by neutralizing the internal fields with the distribution of charge on its outer surface and by reflecting any external electromagnetic radiation. The magnetic susceptibilities of the test bodies will be nearly zero, and photoionization can impart only very minute charges to the test bodies, even in the high-vacuum conditions existing at the proposed altitude of the experiment. The two following paragraphs show that electromagnetic forces on the particle will be at least 9 orders of magnitude smaller than the gravitational force due to the shepherd.

The charge on the test bodies could be zeroed by grounding them to the capsule occasionally. Photoionization by the tracking lasers can be avoided simply by using wavelengths longer than ultraviolet (assuming alkali and alkaline-earth metals will not be used). Cosmic-ray showers are capable of imparting charge to the test bodies, but only if an *incomplete* shower strikes the body, since a complete shower has zero net charge. The cross section for impact of an incomplete shower is roughly $\pi[(r_b+r_c)^2-(r_b-r_c)^2]=4\pi r_b r_c$, where r_b and r_c are the radii of the test body and of the comic-ray shower cone at impact. Assuming that the flux of very high-energy protons and alphas, capable of producing showers of $N=10^5$ particles, is $\sim 1000/\mathrm{m}^2$ day and that the shower cone angle is typically 0.02 rad [56] and that the average distance from shower origin to the test body is 2 m, then roughly 40 000 incomplete showers will strike the shepherd in one year. Assuming, as a worst case, that the charged particles are randomly distributed over the cone and that half of each shower strikes the shepherd, then the charge imparted by one shower will be $\sim\pm\frac{1}{4}e\sqrt{N}$, or $\sim\pm 80$ e. The random walk resulting from 40 000 such showers would impart $\sim\pm 16\,000$ e ($\sim 3\times 10^{-15}$ C) to the shepherd in a year. About one-tenth as much charge would be accumulated by the particle in a year. Therefore after one year the ratio of the Coulomb force to the gravitational force between the test bodies is $(1/4\pi\varepsilon_0)(qQ/mMG)\sim 2\times 10^{-12}$. This is of course negligible. The force due to induced surface charge on the capsule wall may be several orders of magnitude larger, which is still negligible (moreover, this force will usually be nearly perpendicular to the gravitational force between the test bodies). As a worst case for the effect of induced charge, assume that the particle is only 10 cm from the cylinder side wall, which allows the wall to be approximated as a plane. By the method of images, the force is the same as that due to an equal image charge located 10 cm outside the cylinder [57]. Taking the charge on the particle again as $\sim 3\times 10^{-16}$ C, the resulting force will be 2×10^{-10} N, which is 9 or 10 orders of magnitude below the gravitational force between the test bodies when separated by 10 m.

If a test body has nonzero magnetic susceptibility and any dipole moment, then it will experience a torque from the Earth's magnetic field and a force from the field gradient. The torques are of little concern because they affect only rotational motion. The maximum radial gradient of the magnetic field occurs at the poles and is $\partial\mathbf{B}/\partial z\sim 1.2\times 10^{-11}$ T/m at the altitude of one-fourth Earth radius [58]. Assuming that the magnetic susceptibilities can be made less than 10^{-5}, then the magnetic field gradient near the poles will exert a force of $\mathbf{m}\cdot\partial\mathbf{B}/\partial z<9\times 10^{-17}$ N on the shepherd and $<1.8\times 10^{-20}$ N on the particle. The last number is smaller by a factor of 5×10^{-10} than the gravitational force of the shepherd on the particle at a separation of 10

m, and the average of the magnetic force over one orbit is much smaller still.

In case further consideration reveals that charge or magnetization might be substantially larger than indicated above, then other strategies are possible: Small needles could be attached to the surfaces of the test bodies to discharge them (the needles could be in recessed spaces to avoid breakage in handling) [56]. Moreover, low-intensity, low-frequency ac fields could be applied by the steering coils at the beginning and end of each encounter to check for possible charge accumulation or magnetization.

Finally, it should be noted that small, *constant* charges on the test bodies would not vitiate the test of the inverse-square law, since the charge would essentially mimic a slightly different value of G.

VI. PRELIMINARY ERROR BUDGET

For the determination of G, the mass error of the shepherd will probably be the single worst systematic error if it is about 3 parts in 10^7 as expected. The discussion and calculations above indicate that several other effects may reach the level of one part in 10^7 for the G determination. G goes as the square of most of the quantities to be measured. The likely overall error for G is therefore

$$\Delta G/G \sim 1\times 10^{-6} .$$

The shepherd mass error makes no contribution to the error in the test of the inverse-square law at intermediate distances, as inferred from the interaction of the particle with the shepherd [Eq. (6)]. Rather, this test depends on the apparent variation of the *product MG* with separation s. That is, the question is essentially how accurately the relative accelerations of the particle and the shepherd can be measured. We assume that all other errors (which total <1 part in 10^6) still apply undiminished. Thermal effects and uncertainties in the capsule gravitational field are expected to be the limiting errors for this test. Near the most sensitive value of Λ, viz. $\Lambda \sim 3.4$ m, the upper bound on α, as inferred from the interaction of the particle with the shepherd, will be

$$|\alpha| < 1.2\times 10^{-6} .$$

Note that α sensitivity varies greatly with assumed Λ (Fig. 1).

The test of the inverse-square law at distances of the order of an Earth radius, as inferred from perigee precession [Eqs. (8)–(13)] is also unaffected by shepherd mass errors. Moreover, capsule mass anomalies will also have very little effect in this test because the cycloids occur at a wide range of locations throughout the capsule. Every SEE encounter will have some 30 to 40 cycloids. More importantly, we can choose at will the stationary points of the cycloid centroid for a given SEE encounter. Thus, this test is limited principally by the horizontal distance accuracy χ, which in turn is determined chiefly by thermal effects and horizontal distance resolution. We estimate that χ is $\sim 2.5\times 10^{-7}$ m, which is equivalent to assuming a tenfold degradation of accuracy compared to resolution. When $\Lambda \sim 3900$ km, its most sensitive value for this test, the upper bound on α, as inferred from the interaction of the Earth with the test bodies, will be

$$|\alpha| < 4\times 10^{-7} .$$

Note again that the bound varies sharply with the assumed value of Λ.

Information from tangential range rates may also be useful in placing bounds on Λ at distances on the order of one Earth radius. The available precision of $\sim 5\times 10^{-15}$ suggests the possibility of a very sensitive test of Kepler's second law, and hence, the inverse-square law.

The equivalence-principle test based on the interaction of the particle with the shepherd [Eq. (7)] will be relatively immune to systematic errors, provided they remain constant, since the objective is to *compare* the forces on two different bodies in search of a possible difference. That is, *repeatability* is the key. In particular, biases in particle-position determination and errors in the gravitational field due to the capsule will be irrelevant provided the *same trajectory* is used by both particles. (In contrast, the determination of G and the tests of the inverse-square law require a variety of trajectories to map the potential fields of the capsule and the shepherd *in situ*. This is neither necessary nor desirable when testing the equivalence principle.) To arrive at an estimate of the sensitivity of the equivalence-principle test based on the interaction between the two test bodies [Eq. (7)], we first note that the shepherd mass makes no contribution, and we then arbitrarily assume that, of all the remaining systematic errors (which total $<1\times 10^{-6}$), half cannot be eliminated by repeatability. Therefore the upper limit on the composition-dependent differences in α, for $\Lambda > 5$ m, based on the interaction of the *shepherd* with various particles, is, assuming a null result,

$$|\Delta\alpha| < 5\times 10^{-7}$$

and hence

$$|\alpha| < \sim 5\times 10^{-4} .$$

We believe this estimate is conservative. Again we have taken $|\alpha| \sim 10^3 |\Delta\alpha|$ to reflect the packing fraction variation, assuming the mixing angle is $\theta \sim \pi/4$, as explained in Sec. I above. Thus, the limits on α are model dependent, but those on $\Delta\alpha$ are essentially model independent.

The equivalence-principle test based on the interaction of the test bodies with the Earth using Kepler's third law [Eq. (15)] entails a simpler and substantially more favorable error situation. Here the problem is essentially to compare the anomalistic *periods* and *orbital radii* of the two test bodies very accurately. The gravitational attraction of the other test body and of the capsule *per se* is of no consequence because it is a small perturbation with negligible uncertainty. Since the distance between the bodies is monitored continuously to fractional optical wavelengths, the difference in periods is also known with negligible uncertainty (a few parts in 10^{15}). The error in the difference in orbital radii Δr is limited by the capsule-orientation error, which will be known to 0.1 μrad. Therefore the difference of orbital radii will be

known to ~ 1 μm, which is 125 parts in 10^{15}. Thus the relative values of the apparent GM_{Earth}, as determined from Kepler's third law [Eq. (15)], are known to ~ 4 parts in 10^{13}. Therefore the upper limit on the composition-dependent differences in α, for $\Lambda > R_{\text{Earth}}$, based on the interaction of the *Earth* with the shepherd and various particles, is, assuming a null result,

$$|\Delta\alpha| < 4\times 10^{-13}$$

and hence

$$|\alpha| < \sim 4\times 10^{-10} .$$

That is, the equivalence principle will be tested to 4 parts in 10^{13} for $\Lambda > R_{\text{Earth}}$. Please see "Note added in proof."

VII. CONCLUSION

The satellite energy exchange (SEE) method promises major advances in the long-standing measurement problems of Newtonian gravitation—the determination of G, the validation of the inverse-square law and of the equivalence principle, and possibly also a measurement of $\dot{G}$. Three characteristics of the SEE method basically account for its great accuracy.

(1) *The great sensitivity with which orbital perturbations can be detected.* The almost legendary ability of orbital mechanics to measure small perturbations is well known, most notably in this century through the precession of Mercury's perihelion, and more recently through the extremely precise satellite geodesy work in the 1960's and 1970's, through recent tests of the inverse-square law at distances of planetary orbits and planetary flybys, and through ongoing tests of general relativity. The SEE method is a natural outgrowth of this heritage. It is based on the assumption that it is better to accept the known large forces as they are and find ways to measure minute departures from them, rather than to focus on artificially constructed small forces and try to suppress the effects of the large forces. That is, the SEE method accepts the fact that the two masses are preponderantly in *Earth* orbits, and its *modus operandi* is simply to observe their perturbation.

(2) *The scale of the experiment.* The most obvious benefits of the scale are the excellent distance resolution and the effectively unlimited time resolution. In addition, the large distance scale inherently mitigates the effects of any shepherd mass anomalies, and SEE's unique ability to vary the separation of the test masses over a wide range allows the ideal combination of (a) very close encounters to map the field of the shepherd and (b) larger separations for measuring the interactions of interest. The distance scale also corresponds neatly with the intermediate-range gap in Λ where the limits on α are poorly known. Finally, the encounter durations are short enough to allow several hundred SEE encounters during the life of the satellite, which will reduce random experimental errors by an order of magnitude.

(3) *The low-noise level.* The inherent potential of space as a low-noise environment will be realized chiefly by choosing a capsule orbit which minimizes drag and keeps solar radiation absorption nearly constant, and by using jerk-free methods to control the position and attitude of the capsule during SEE encounters (especially using solar radiation pressure to "sail" the capsule and using torques from Earth's magnetic field to orient it). In testing the inverse-square law and the equivalence principle, the SEE method is unique in working at *intermediate* distances without being forced to rely on assumptions about the location and compositions of the nearby rocks, soil, and basements, which terrestrial experiments must do. A final salient advantage of the SEE method is that it uses no mechanical devices or electric fields to constrain the test masses, which is of enormous import in measuring a force so weak as gravity. Rather, the SEE method simply observes the natural orbital motion.

To capitalize on these three characteristics, an orbital configuration is necessary which can be confined within a satellite and which evolves over a fairly long time. The encounter phase of a horseshoe orbit meets these requirements admirably. With it, the relative motion of both bodies can take place within a long narrow cylinder, over a period of several days. Most importantly, in the SEE method the interacting bodies can be observed essentially *free of other (nongravitational) forces.*

Note added in proof. It may be possible to test the equivalence principle (EP) to ~ 1 part in 10^{15}, at separations $\sim R_{\text{Earth}}$ (Test 5) by using a different experimental configuration during this EP test. This would lower the curve "SEE-Kepler-EP" (Fig. 1) 2 or 3 orders of magnitude. The new configuration entails (1) spinning the capsule about its long axis, (2) maintaining quasi-inertial orientation of this axis, (3) keeping the shepherd caged at one end of the capsule, and (4) placing two particles in slightly different earth orbits near the capsule center of mass. This configuration is favorable because it improves the vertical distance resolution and obviates the need for extremely accurate pitch determination.

ACKNOWLEDGMENTS

The authors express their appreciation to the many individuals without whose contributions our work would have been much more difficult if not impossible. We thank George Gillies and his colleagues Steve Allison and Rogers Ritter for seminal advice at the outset of our work, drawing on their long experience in the art of G determinations; Eric Black and Mark Rupright for their assistance in calculations and derivations; Ed Harris, Clarence Wingate, Peter Bender, John Junkins, Gabriel Luther, and Richard Cohen for their patience in reviewing the manuscript and for insightful discussions and suggestions; and George Bush and Harold Black for their unflagging encouragement and their wisdom. This work was supported in part by the Tennessee Higher Education Commission Center of Excellence Science Alliance.

[1] E. R. Cohen and B. N. Taylor, Phys. Today **40** (8), 11 (1987); CODATA Bull. **63**, 12 (1986).
[2] G. T. Gillies, *Gravitational Measurements, Fundamental Metrology, and Constants* (Kluwer Academic, New York, 1988), pp. 191–214.
[3] H. de Boer, in *Precision Measurement and Fundamental Constants II,* edited by B. N. Taylor and W. D. Phillips, Natl. Bur. Stand. Special Publ. 617 (National Bureau of Standards, Washington D.C., 1984).
[4] G. T. Gillies, Am. J. Phys. **58**, 525 (1990).
[5] Y. Avron and M. Livio, Astrophys. J. **304**, L61 (1986); D. Berman and R. Forward, Adv. Astron. Sci. **24**, 95 (1969); P. Farinella *et al.,* Astrophys. Space Sci. **73**, 417 (1980); R. L. Forward, *Research Toward Feasibility of an Instrument of Measuring Gradients of Gravity* (Hughes Research Corp., Malibu, CA, 1966); J. G. Hills, Astron. J. **92**, 986 (1986); Anna M. Nobili *et al.,* ESA J. **14**, 389 (1990); R. C. Ritter and G. T. Gillies, University of Virignia report, 1981 (unpublished) J. P. Vinti, Celestial Mechanics **5**, 204 (1972); L. S. Wilk, ed., *Studies of Space Experiments to Measure Gravitational Constant Variations and the Eötvös Ratio* (Measurement Systems Laboratory, MIT, Cambridge, MA, 1971).
[6] L. Facy and C. Pontikis, C. R. Acad. Sci. Paris **272**, 1397 (1971); O. V. Karagioz *et al.*, Phys. Zemli **12**, 106 (1976) [Phys. Solid Earth **12**, 351 (1976)]; G. G. Luther and W. R. Towler, Phys. Rev. Lett. **48**, 121 (1982); M. U. Sagitov *et al.,* Dokl. Akad. Nauk SSSR **245**, 567 (1979) [Sov. Phys. Dokl. **245**, 20 (1981)].
[7] C. Stubbs, in *Proceedings of the XXIV International Conference on High Energy Physics,* Munich, West Germany, 1988, edited by R. Kotthaus and J. Kuhn (Springer-Verlag, Berlin, 1988), pp. 1325–1331.
[8] W. M. Fairbank, in *Searches for New and Exotic Phenomena,* Proceedings of the Twenty-Third Rencontre de Moriond, Les Arcs, France, 1988, edited by O. Fackler and J. Tran Thanh Van (Editions Frontières, Gif-sur-Yvette, 1988).
[9] F. P. Calaprice, in *Fifth Force and Neutrino Physics,* Proceedings of the Twenty-fourth Rencontre de Moriond, Les Arcs, France, 1989, edited by O. Fackler and J. Tran Thanh Van (Editions Frontières, Gif-sur-Yvette, 1989).
[10] P. E. Boynton *et al.,* Phys. Rev. Lett. **59**, 3 1385 (1987); D. H. Eckhardt *et al., ibid.* **60**, 2567 (1988); E. Fischbach *et al., ibid.* **56**, 3 (1986); F. D. Stacey *et al.,* Rev. Mod. Phys. **59**, 157 (1987); P. Thieberger, Phys. Rev. Lett. **58**, 1066 (1987).
[11] Y. Fujii, Nature Phys. Sci. **234**, 5 (1971); Ann. Phys. (N.Y.) **69**, 494 (1972); D. R. Long, Nature (London) **260**, 417 (1976); R. E. Spero *et al.,* Phys. Rev. Lett. **44**, 1645 (1980); D. R. Long, Nuovo Cimento **55B**, 252 (1984); Y. T. Chen *et al.,* Proc. R. Soc. London **A394**, 47 (1984).
[12] E. Fischbach and C. Talmadge, Mod. Phys. Lett. A **4**, 2303 (1989); Nature (London) **356**, 207 (1992).
[13] C. M. Will, Science **250**, 770 (1990).
[14] D. F. Bartlett and W. L. Tew, Phys. Rev. Lett. **63**, 1531 (1989); S. Y. Chu and R. H. Dicke, *ibid.* **57**, 1823 (1986); D. H. Eckhardt, *ibid.* **57**, 2868 (1986); C. Jeckeli *et al., ibid.* **64**, 1204 (1990); Y. E. Kim, Phys. Lett. B **195**, 245 (1987).
[15] E. G. Adelberger, Phys. Rev. Lett. **59**, 849 (1987).
[16] E. G. Adleberger *et al.,* Phys. Rev. D **42**, 3267 (1990).
[17] P. Fayet, Phys. Lett. B **227**, 127 (1989); R. D. Pecci, J. Sola, and C. Wetterich, *ibid.* **195**, 183 (1987).
[18] A. de Rújula, Phys. Lett. B **180**, 213 (1986).
[19] G. W. Gibbons and B. F. Whiting, Nature (London) **291**, 636 (1981).
[20] See, for example, T. D. Lee and C. N. Yang, Phys. Rev. **98**, 1501 (1955).
[21] V. B. Braginsky and V. I. Panov, Zh. Eksp. Teor. Fiz. **61**, 873 (1971) [Sov. Phys. JETP **34**, 463 (1972)]; P. G. Roll, R. Krotkov, and R. H. Dicke, Ann. Phys. (N.Y.) **26**, 442 (1964).
[22] R. Battiston, in *Searches for New and Exotic Phenomena,* Proceedings of the Twenty-Third Rencontre de Moriond, Les Arcs, France, 1988, edited by O. Fackler and J. Tran Thanh Van (Editions Frontieres, Gif-sur-Yvette, 1988).
[23] ESA and NASA, "STEP: Satellite Test of the Equivalence Principle; Assessment Study Report" [ESA Ref: SCI(90)], 1991.
[24] P. A. M. Dirac, Nature (London) **139**, 323 (1937); Proc. R. Soc. London **A165**, 199 (1938).
[25] William J. Marciano, Phys. Rev. Lett. **52**, 489 (1984).
[26] See Gillies, Refs. [2] and [3], and references therein.
[27] G. H. Darwin, Acta Math. **21**, 99 (1897).
[28] S. F. Dermott and C. D. Murray, Icarus **48**, 1 (1981).
[29] C. F. Yoder, G. Colombo, S. P. Sinnot, and K. A. Yoder, Icarus **53**, 431 (1983).
[30] See, for example, Herbert Goldstein, *Classical Mechanics* (Addison-Wesley, New York, 1950).
[31] B. Lange, Am. Inst. Aeronaut. Astronaut. J. **2**, 1590 (1964).
[32] Staff of Space Dept., Johns Hopkins U., Applied Physics Lab., and Staff of Guidance and Control Lab., Stanford U., J. Spacecraft Rockets **11**, 637 (1974).
[33] A. J. Sanders and E. D. Black (unpublished).
[34] These include compensation schemes which also remove the gradients of the Earth's field. See R. L. Forward, Phys. Rev. D **26**, 735 (1982); Richard Friedberg, *ibid.* **36**, 386 (1986).
[35] See, for example, P. R. Heyl, U.S. Bur. Stand. J. Res. **5**, 1243 (1930); P. R. Heyl and P. Chrzanowski, J. Res. Natl. Bur. Standards **29**, 1 (1942). However, cylinders introduce large nonlinearities in the period of a Cavendish pendulum due to the extreme proximity of the masses required in laboratory experiments; see A. H. Cook and Y. T. Chen, J. Phys. A **15**, 1591 (1982).
[36] A. H. Cook, Contemp. Phys. **9**, 227 (1968).
[37] J. L. MacArthur and A. S. Posner, IEEE Trans. Geoscience Remote Sensing **GE-23**, 517 (1985).
[38] For a review, see W. E. Deeds and C. V. Dodd, in *Pressure Vessels and Piping Technology—1985—a Decade of Progress* (ASME, New York, 1985), and references therein.
[39] See, for example, Jean Kovalevsky, *Introduction to Celestial Mechanics* (Springer-Verlag, New York, 1963).
[40] H. D. Black (private communication).
[41] W. N. Hess, *The Radiation Belt and Magnetosphere* (Ginn Blaisdale, Waltham, MA, 1968).
[42] P. J. Nawrocki and Robert Papa, *Atmospheric Processes* (Prentice-Hall, Englewood Cliffs, NJ, 1963).
[43] Committee for the COSPAR International Reference Atmosphere (CIRA) of COSPAR Working Group **4**, CIRA 1972 (Akademie Verlag, Berlin, 1972).
[44] V. B. Braginsky and A. B. Manukin, *Measurement of Weak Forces in Physics Experiments* (University of Chicago Press, Chicago, 1977).
[45] *AXIOM 2/20 Operations Manual* (Zygo Corporation, 1989), Chap. 10; see also Hewlett Packard stock number

HP 5527 and Spindler & Hoyer stock numbers 04 322, 04 0323, 04 0365, and 04 0366.
[46] E. Debler, Metrologia **28**, 85 (1991).
[47] C. Braun, Denkschr. Akad. Wissenschaft Wien, Math. Naturwissenschaftliche Klasse **64**, 187 (1897).
[48] See, for example, A. H. Cook, in *Three Hundred Years of Gravitation,* edited by S. W. Hawking and W. Israel (Cambridge University Press, Cambridge, England, 1987).
[49] R. Schoonover (private communication). Early in 1991 Dr. Schoonover also told the authors it was his opinion that large-mass comparators accurate to 1 part in 10^6 could be built with current technology. PTB's recent publication amply substantiates Dr. Schoonover's judgment.
[50] G. T. Gillies (private communication).
[51] L. W. Alvarez, Phys. Today **40**, 24 (1987).
[52] C. A. Wingate (private communication).
[53] Frank Colucci, Space **6**, 1 (1990); Ithaco, Inc., PADS: Precision Attitude Determination System, Technical Description (Report 93172, Rev. E), 1989.
[54] Sun-Angle Sensors Short-Form Catalogue (Adcole Corporation); Richard S. Warner (private communication).
[55] M. Froeschle and F. Mignard, Appl. Opt. **20**, 3251 (1981).
[56] D. T. King (private communication).
[57] See W. R. Smythe, *Static and Dynamic Electricity,* 3rd ed. (McGraw-Hill, New York, 1968), Sec. 5.299 for an exact expression for the Green's function for a cylindrical box.
[58] See, for example, J. K. Hargreaves, *The Upper Atmosphere and Solar-Terrestrial Relations* (Van Nostrand Reinhold, New York, 1979).

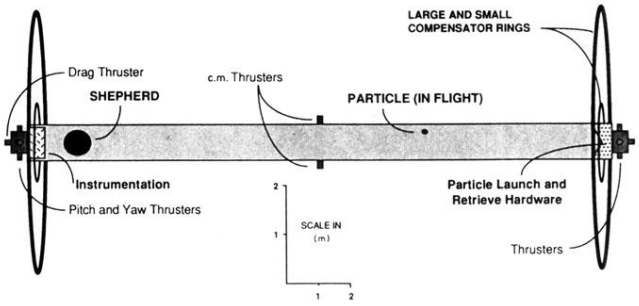

FIG. 6. Diagram of the capsule containing the "shepherd," "particle," and instrumention. The large rings on the ends cancel the internal gravitational field of the cylinder itself and of the instrumentation (vertical scale magnified $\times 1.5$ for clarity).

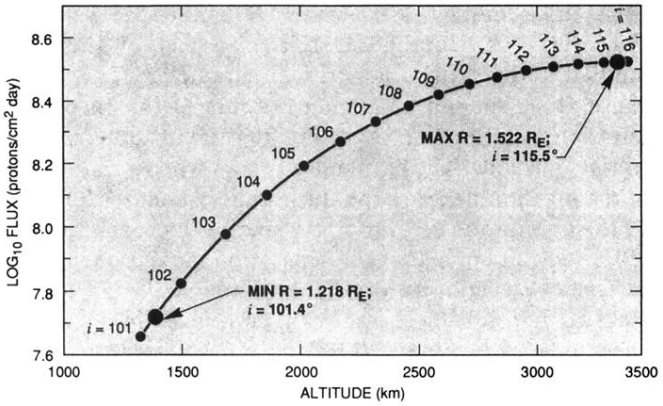

FIG. 7. Circular-orbit integrated flux (COIF) of high energy (>34 MeV) protons for continuous-sunlight orbits. To be in continuous sunlight, orbits must have altitudes between 1390 and 3330 km and inclinations between 101.4° and 115.5°. The 3330-km orbit has about six times the high-energy flux of the 1390-km orbit (from Eq. (16), including Eq. (17), and Fig. 9 of Appendix II of Hess [41]).